COMMUNICATIONS

Time-resolved photoelectron imaging of the photodissociation of I_2^-

Alison V. Davis, Roland Wester,[a] Arthur E. Bragg, and Daniel M. Neumark
Department of Chemistry, University of California, Berkeley, California, 94720
and Chemical Sciences Division, Lawrence Berkeley National Laboratory, Berkeley, California, 94720

(Received 3 October 2002; accepted 19 November 2002)

Time-resolved photoelectron imaging is presented as a new method for the study of anion dynamics. Time-dependent photoelectron energy spectra and angular distributions are extracted from images taken during the dissociation of I_2^- at 793 nm, and used to follow in detail the dissociation dynamics from 0–1 ps. © *2003 American Institute of Physics.* [DOI: 10.1063/1.1536617]

Time-resolved photoelectron spectroscopy (TRPES) is a powerful technique in which one measures the photoelectron spectrum of a species electronically excited by a pump laser pulse as a function of pump–probe delay.[1–3] The time-dependent photoelectron kinetic energy (eKE) distribution probes the nonstationary excited and ground state dynamics induced by the pump pulse, enabling one to follow the dynamics of diverse processes such as dissociation, vibrational relaxation, and radiationless transitions. TRPES has been applied to anions and neutrals; since anions can be mass-selected and photodetached at much lower photon energies than neutrals, they are particularly attractive targets for TRPES.

Most TRPES studies performed to data have used time-of-flight (TOF) analysis to determine the eKE distribution. However, photoelectron imaging offers comparable or better energy resolution, while also yielding the evolving photoelectron angular distribution (PAD). Time-resolved photoelectron imaging (TRPEI) has been implemented for neutral systems; recent reviews by Suzuki and Whitaker[4] and Seideman[5] stress the experimental and theoretical aspects respectively. For anions, photoelectron imaging without time resolution has been applied to W_n^- and C_n^- clusters by Baguenard *et al.*,[6,7] and to CS_2^- and $OCS^-(H_2O)_{1,2}$ by Surber and Sanov.[8] Here we report the first application of TRPEI to a negative ion, in which we investigate the time dependence of the photoelectron energy and angular distribution of I_2^- as it dissociates to $I^- + I$. The results presented here show surprising changes in the PADs at delay times for which the interaction between the recoiling fragments is exceedingly weak.

Previously, we have developed potentials for the ground $\tilde{X}^2\Sigma^+_{u,1/2}$ and excited $\tilde{A}'^2\Pi_{g,1/2}$ states of I_2^- using conventional and time-resolved PES.[9–13] Relevant anion and neutral potentials and the pump–probe scheme for the experiment are shown in the top part of Fig. 1. Our initial study[9] of excitation to the $\tilde{A}'^2\Pi_{g,1/2}$ state showed that dissociation, as measured by the appearance of I^- photoproduct, takes about 300 fs. A subsequent higher-resolution study[10] revealed a small shift in the spectra over the period 320–720 fs, indicating the presence of a shallow well at long range on the excited potential. Because of its relatively simple and well-characterized dynamics, I_2^- makes an ideal system for the first anion TRPEI experiments, which yield new information on the evolution of the PAD during dissociation.

The experimental apparatus, shown in the bottom part of Fig. 1, consists of a femtosecond laser and a pulsed anion source/mass spectrometer with a new photoelectron imaging detector; the latter replaces a magnetic bottle TOF spectrometer used in earlier studies on this instrument.[14] I_2^- is formed in the source region of the apparatus (labeled "A" in Fig. 1), where a pulsed expansion of argon over crystalline I_2 is crossed by the beam from an electron gun. The anions are injected into a Wiley–McLaren mass spectrometer at a beam energy of ~1500 V, and intersect the pump and probe laser pulses after 2 regions of differential pumping.

In the photoelectron imaging detector, the anion packet is rereferenced to a negative potential, typically −2500 V, within a pulsed rereferencing tube ("B") that also serves as a mass gate. A few millimeters after exiting the tube, the anions are intercepted by the pump and probe laser pulses between in-line extraction plates in the velocity-map configuration.[15] The photoelectrons are detected on a 70-mm dual microchannel plate stack with a phosphor screen ("D"); the microchannel plates lie 60 cm downstream from the extraction plates. The microchannel plates are gated on only near the electron arrival time to reduce noise and eliminate detection of neutral molecules. At a much later time, any undetached ions are redirected by a pulsed deflector ("C") to a small retractable microchannel plate detector with which ion intensity is monitored.

Photoelectron imaging provides 100% photoelectron collection efficiency. In addition, Doppler broadening effects associated with using a magnetic bottle with a fast negative ion beam are eliminated,[16] yielding better photoelectron energy resolution than was ever achieved with the magnetic bottle on this instrument, even when the anions were slowed down by pulsed deceleration. The coaxial velocity map imaging geometry in Fig. 1 has several advantages over the

[a]Current address: MPI für Kernphysik, Postfach 103980, 69029 Heidelberg, Germany.

perpendicular arrangement used elsewhere;[6,8] in particular, the position and energy resolution of the photoelectrons are independent of the ion beam energy and energy spread.

The photoelectrons are imaged at 50 Hz by a Dalsa 1M30 digital camera (''E''). A desktop computer determines the center of each electron impact in real time by calculating the average position of each cluster of illuminated pixels. This procedure increases the resolution over simple integration of the electron image, but can lead to saturation effects if the photoelectron density is high enough that the clusters overlap. In the I_2^- spectra presented here, such saturation is minimal in the energy region examined.

The laser is a commercial Ti:Sapphire system (Clark-MXR; output 1 mJ at 793 nm, 90 fs pulses, 500 Hz). Part of the fundamental (70 μJ) is used to pump the dissociative $\tilde{A}'^2\Pi_{g,1/2}$ state of I_2^-. The remainder is frequency-tripled to produce a 20 μJ pulse at 265 nm, and this serves as the probe photodetachment pulse. The pump–probe delay is varied by means of a translation stage. The beams are combined and collinearly focused into the interaction region of the spectrometer. The polarization vectors of the pump and probe are parallel to each other and to the detector plane. The zero-of-time was determined by comparing the time-dependent growth of I^- features from the dissociation of I_2^- to the known I^- rise time.[10]

The image obtained with the probe pulse only (i.e., the I_2^- photoelectron spectrum at 265 nm) is shown in Fig. 2(a). The laser polarization direction is vertical in the plane of the page. The image has been 4-way symmetrized, and scaled amounts of noise due to the probe laser and to collisional photodetachment of the ions have been subtracted. Additionally, the y-axis of the image has been scaled by 0.98 to compensate for a slight distortion, caused by charging of the ion optics that shortens the image in the x-direction. These corrections have been made to all images presented here. Figure 2(b) shows a slice through the reconstructed photoelectron velocity distribution, determined using the basis-set expansion method (BASEX) of Reisler and co-workers.[17] Larger radii correspond to faster electrons; four rings of intensity which are apparent in the nontransformed image are clearly defined in the velocity distribution. In Fig. 2(c), the angle-integrated photoelectron spectrum from the velocity slice is shown. The photoelectron intensity is plotted versus the electron kinetic energy (eKE); this and all energy spectra were calibrated with the known photoelectron energy for detachment of I^-. The detailed assignment of the I_2^- PE spectrum has been discussed elsewhere.[13] The peaks are due to detachment to the several states of neutral I_2 labeled in Fig. 2(c), some of which are shown in the top part of Fig. 1. This spectrum demonstrates the resolution of the imaging detection, which approaches the femtosecond laser bandwidth limit (~40 meV) for low-energy peaks; the spacing between the fully-separated peaks near 0.9 eV is only 85 meV.

Time-dependent pump–probe data are shown in Fig. 3. A scaled amount of probe-only data has been subtracted from the images and spectrum in order to highlight the dynamics on the upper state. Transformed images are shown in Figs. 3(a)–3(c) for three pump–probe delays. At 0 fs, the photoelectrons cover a wide energy and angular range, especially at higher energies. By 100 fs after the pump laser pulse, the distribution has narrowed in energy and looks an-

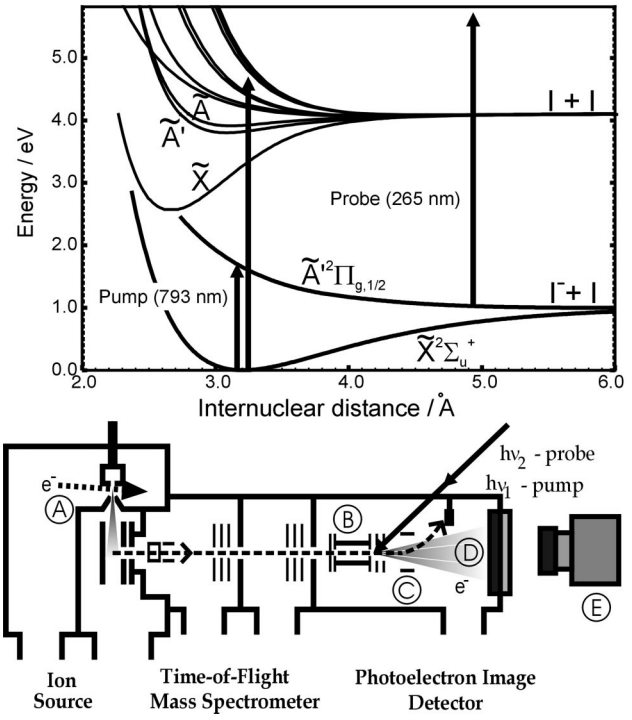

FIG. 1. (Top) Potential energy curves of the $\tilde{X}^2\Sigma_{u,1/2}^+$ and $\tilde{A}'^2\Pi_{g,1/2}$ states of I_2^-, and neutral states which converge to ground state I+I. (Bottom) Schematic of TRPEI apparatus, detailing (A) the ion source, (B) the ion rereferencing and velocity map imaging stack, (C) pulsed deflector, (D) MCP/phosphor screen image detector, and (E) digital camera.

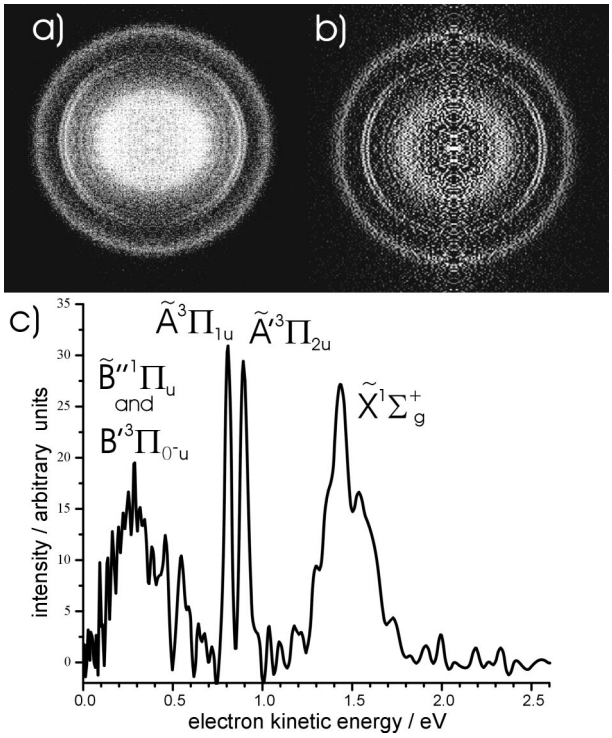

FIG. 2. (a) Photoelectron image of ground state I_2^- detached with 265 nm light. (b) Slice through the reconstructed photoelectron velocity distribution of the image shown in (a). (c) Photoelectron spectrum of ground state I_2^- achieved by angle-integrating the reconstructed image.

isotropic, with more intensity at $\theta=90°$ than at 0°, and two narrow rings have become apparent. By 300 fs, the two rings dominate the image; the intensity of each is clearly peaked at $\theta=90°$. The outer and inner rings correspond to detachment of I^- photoproduct to the ground $^2P_{3/2}$ and spin–orbit excited $^2P_{1/2}$ states, respectively, of atomic iodine. The corresponding angle-integrated energy spectra are plotted on Fig. 3(d) and are in good agreement with our previous results,[9,10] showing broad, transient features at 0 and 100 fs associated with dissociating I_2^- on the $\tilde{A}'\,^2\Pi_{g,1/2}$ evolving into the two atomic I^- features by 300 fs. The widths of the fast and slow atomic peaks at 300 fs are 57 and 40 meV, respectively.

The two atomic peaks shift to higher energy by about 10 meV over the interval from 300–1000 fs. The shift is shown in Fig. 4, where the center of the atomic $^2P_{3/2}$ peak in electron kinetic energy is plotted as a dashed line (y-scale to the right) versus pump–probe delay, and is due to the passage of the wave packet through a shallow, long-range well on the $\tilde{A}'$ excited state, as discussed previously ($R_e=6.2\pm0.6$ Å, $D_e=0.017\pm0.010$ eV).[10] The current study yields a somewhat more complete picture of the effect of this well; we detect an additional shift of ~1 meV after 720 fs, the largest delay studied in the earlier work.

The newest information garnered from the images is the evolution of the PAD as the I_2^- dissociates. In our experiment, excited state anions can be aligned but not oriented by the linearly polarized pump beam, so for each electron kinetic energy, the PAD can be represented by[18,19]

$$\frac{d\sigma}{d\Omega}=\frac{\sigma}{4\pi}[1+\beta_2 P_2(\cos\theta)+\beta_4 P_4(\cos\theta)] \quad (1)$$

where θ is the angle between the electron velocity and laser polarization vectors, and β_{2n} is the anisotropy parameter associated with P_{2n}, the $2n$th Legendre polynomial. Eq. (1) differs from the PAD for one-photon photodetachment of randomly oriented molecules, for which $\beta_4=0$ and $-1\leqslant\beta\leqslant2$.[20]

The parameters β_2 and β_4 are evaluated directly from the matrix coefficients calculated with the BASEX inversion technique, and can be calculated for any energy range. Any changes in β_2 and β_4 over the time scale of our experiment must be associated with dissociation and not with rotational alignment effects, since the time scale for I_2^- dissociation is much shorter than its rotational period. For each spectrum transformed into energy-space via the BASEX method, the anisotropy parameters are evaluated over a range of electron kinetic energies encompassing the higher energy transient feature that ultimately evolves into the atomic peak at 1.6 eV. The boundaries of this range change as a function of delay time, since by calculating β_2 and β_4 for only the feature of interest we avoid convoluting additional noise into the analysis. The results of the calculation of β_2 for two different experimental runs are shown in Fig. 4 as connected points (y-scale to the left). β_4 is not shown, as it was found to be quite small ($|\beta_4|<0.1$) and not particularly time-dependent.

At early times during the dissociation, the β_2 parameter decreases in value from around -0.1 near $t=0$ fs to -0.55 near $t=200$ fs. It stays nearly constant until 350 fs, when it rises, peaking at about -0.44 near 580 fs. This rise is followed by a shallow drop by about 800 fs, after which no significant change occurs. For all images taken with a time delay larger than 800 fs the average value of β_2 is -0.520 ± 0.035. This average value is shown as a diamond at the end of the data in Fig. 4, and its uncertainty should be a reasonable estimate of the error bars associated with the rest of the points. The value of β_2 after 800 fs is the anisotropy parameter for I^-, and reflects the interference of *s*- and *d*-electron partial waves produced in the photodetachment from the atomic *p*-orbital.[20]

The delay times over which β_2 changes show substantial but not complete correlation with those over which the energy distribution evolves. The sharp drop in β_2 during the

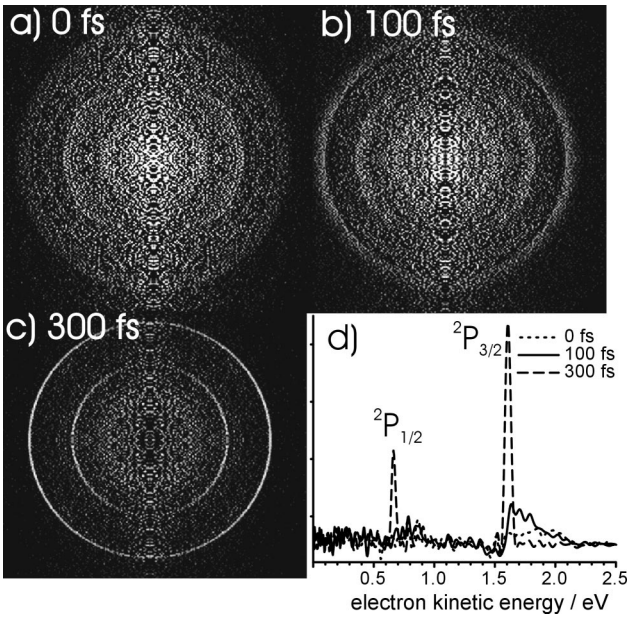

FIG. 3. (a)–(c) Reconstructed photoelectron velocity maps for dissociating I_2^- probed 0, 100, and 300 fs after excitation.

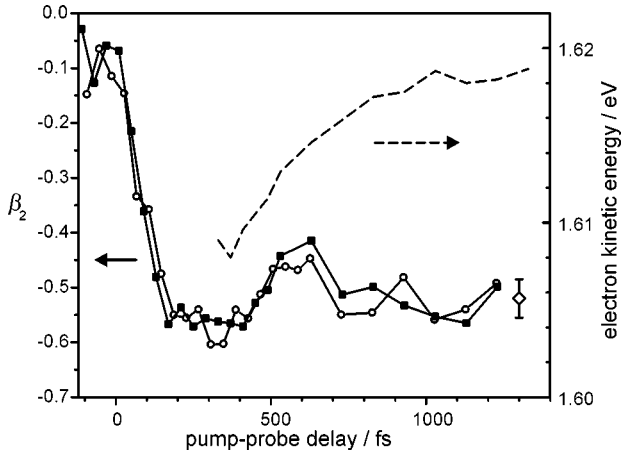

FIG. 4. Connected points, left axis: β_2 as a function of delay between photodissociation and photodetachment lasers. Two separate data sets are shown, demonstrating reproducibility. The right-most point (open diamond) represents an average of all data after 800 fs. Dashed line, right axis: Position in electron kinetic energy of the center of the atomic feature near 1.6 eV, also as a function of delay.

first 200–300 fs occurs while the photoelectron energy spectrum undergoes the most change, from broad transient features at the earliest times to the sharp, I^--like features by 220–300 fs. The value of β_2 reflects the shape of the orbital from which detachment occurs, and this should certainly change as the wave packet traverses the steep part of the anion potential from the Franck–Condon region around $R_e = 3.2$ Å to the vicinity of the shallow well at 6.5 Å. In particular, calculations by Maslen *et al.*[21] and Gellene[22] show that strong mixing with higher-lying $^2\Sigma_g^+$ state occurs as the I–I bond lengthens over this range.

The small increase in β_2 after 350 fs matches the beginning of the shift in the atomic peaks in the energy spectra, which, as discussed above, result from the wave packet moving out of the shallow well in the $\tilde{A}'\,^2\Pi_{g,1/2}$ state. However, the subsequent drop in β_2 around 700–800 fs does not correlate with any equivalent new trend in the photoelectron energy spectra. We suggest that it reflects a change in the character of the orbital in which the electron resides, from an orbital which has equal amplitude on two weakly interacting I atoms to one which is localized on a single I atom, i.e., photodetachment from truly separated $I+I^-$ products. This effect requires mixing between I_2^- potential energy curves with g and u symmetry, which can occur in the asymptotic region where the energy difference between g and u curves correlating to the same product states, such as the $\tilde{A}'\,^2\Pi_{g,1/2}$ and $\tilde{X}\,^2\Sigma_u^+$ curves in Fig. 1, becomes very small. By 800 fs, for example, the two fragments are separated by 13 Å, and the two potential energy curves are separated by only 0.8 meV (6 cm^{-1}). Sources of this mixing include hyperfine coupling terms in the molecular Hamiltonian or external electric fields.[23]

The possible role of external fields is particularly intriguing, since the anions are photodetached in a DC field of around 500 V/cm. Consider a dissociating I_2^- molecule on the $\tilde{A}'\,^2\Pi_{g,1/2}$ state with its axis parallel to the electric field. If I_A and I_B are the I atoms closer to and further from the detector, respectively, then in the absence of any g/u mixing, the overall electronic wave function at long range has g symmetry and is of the form $(1/\sqrt{2})(I_A^-I_B + I_AI_B^-)$. The asymptotic wave functions for which the excess charge is localized on a particular I atom, i.e., $I_A^-I_B$ or $I_AI_B^-$, are obtained from $g \pm u$ linear combinations. In our extraction field, at an internuclear separation of 13 Å, localization of the full negative charge on I_A is about 0.5 cm^{-1} lower in energy than having the charge I_B. This splitting between $g \pm u$ asymptotic states is smaller than but within an order of magnitude of the splitting between the $\tilde{A}'\,^2\Pi_{g,1/2}$ and $\tilde{X}\,^2\Sigma_u^+$ curves at this distance, and we should point out that these curves are not particularly well-determined at such larger distances. In any case, it seems plausible that the extraction field can induce the g/u mixing needed for charge localization.

In summary, we have established the technique of time-resolved photoelectron imaging as a means for studying anion dynamics by examining the dissociation of I_2^-. TRPEI yields excellent energy resolution when compared with TOF methods, and, more importantly, provides literally another dimension for analysis: the evolution of the photoelectron angular distribution as the I_2^- dissociates. Although we have not quantitatively analyzed the evolving PAD, we have shown that the anisotropy of the ejected photoelectrons is a sensitive probe of the dissociation process that, at the very least, complements the time-evolving PE spectra. In addition, the evolution of the PAD at very long times provides new information on the dissociation dynamics which we propose is due to localization of the excess electron on one of the I atoms. We thus expect TRPEI to be an important new technique that will be applicable to a host of problems in anion dynamics.

This work is supported by the National Science Foundation under Grant No. CHE-0092574. A.E.B. is an NSF predoctoral fellow. R.W. acknowledges support from the Alexander von Humboldt-Stiftung and from the Emmy Noether-Programm of the Deutsche Forschungsgemeinschaft.

[1] I. Fischer, D. M. Villeneuve, M. J. J. Vrakking, and A. Stolow, J. Chem. Phys. **102**, 5566 (1995).
[2] D. R. Cyr and C. C. Hayden, J. Chem. Phys. **104**, 771 (1996).
[3] D. M. Neumark, Annu. Rev. Phys. Chem. **52**, 255 (2001).
[4] T. Suzuki and B. J. Whitaker, Int. Rev. Phys. Chem. **20**, 313 (2001).
[5] T. Seideman, Annu. Rev. Phys. Chem. **53**, 41 (2002).
[6] B. Baguenard, J. C. Pinare, C. Bordas, and M. Broyer, Phys. Rev. A **6302**, 3204 (2001).
[7] B. Baguenard, J. C. Pinare, F. Lepine, C. Bordas, and M. Broyer, Chem. Phys. Lett. **352**, 147 (2002).
[8] E. Surber and A. Sanov, J. Chem. Phys. **116**, 5921 (2002).
[9] B. J. Greenblatt, M. T. Zanni, and D. M. Neumark, Chem. Phys. Lett. **258**, 523 (1996).
[10] M. T. Zanni, V. S. Batista, B. J. Greenblatt, W. H. Miller, and D. M. Neumark, J. Chem. Phys. **110**, 3748 (1999).
[11] M. T. Zanni, A. V. Davis, C. Frischkorn, M. Elhanine, and D. M. Neumark, J. Chem. Phys. **112**, 8847 (2000).
[12] M. T. Zanni, B. J. Greenblatt, and D. M. Neumark, J. Chem. Phys. **109**, 9648 (1998).
[13] M. T. Zanni, T. R. Taylor, B. J. Greenblatt, B. Soep, and D. M. Neumark, J. Chem. Phys. **107**, 7613 (1997).
[14] B. J. Greenblatt, M. T. Zanni, and D. M. Neumark, Faraday Discuss. **108**, 101 (1998).
[15] A. T. J. B. Eppink and D. H. Parker, Rev. Sci. Instrum. **68**, 3477 (1997).
[16] O. Cheshnovsky, S. H. Yang, C. L. Pettiette, M. J. Craycraft, and R. E. Smalley, Rev. Sci. Instrum. **58**, 2131 (1987).
[17] V. Dribinski, A. Ossadtchi, V. A. Mandelshtam, and H. Reisler, Rev. Sci. Instrum. **73**, 2634 (2002).
[18] D. J. Leahy, K. L. Reid, and R. N. Zare, J. Chem. Phys. **95**, 1757 (1991).
[19] K. L. Reid and J. G. Underwood, J. Chem. Phys. **112**, 3643 (2000).
[20] J. Cooper and R. N. Zare, J. Chem. Phys. **48**, 942 (1968).
[21] P. E. Maslen, R. Faeder, and R. Parson, Chem. Phys. Lett. **263**, 63 (1996).
[22] S. B. Sharp and G. I. Gellene, Mol. Phys. **98**, 667 (2000).
[23] P. R. Bunker, *Molecular Symmetry and Spectroscopy*, 2nd ed. (NRC Research, Ottawa, 1998).